I&EC research
Industrial & Engineering Chemistry Research

Article

pubs.acs.org/IECR

Operation-Region-Decomposition-Based Singular Value Decomposition/Neural Network Modeling Method for Complex Hydraulic Press Machines

XinJiang Lu,* YiBo Li, and MingHui Huang

State Key Laboratory of High Performance Complex Manufacturing and School of Mechanical & Electrical Engineering, Central South University, Hunan 410083, China

ABSTRACT: Hydraulic press machines (HPMs) are a complex nonlinear system that work across a large operation region. In such a region, input/output samples do not easily satisfy the requirements of data-driven modeling because of many practical constraints involved. This renders HPMs difficult to model accurately. In this paper, an operation-region-decomposition-based SVD/NN modeling method is proposed for this type of system. It can produce models that work across a large operation region without input spectra with special properties. Using this method, this operation region is first broken down into a group of local operation regions. Every local region is excited by its corresponding input signal. Because the complexity of the system at the local region is much lower than the original system throughout the operation region, the required input signal for modeling at a local region is easier to obtain than the one suitable for the whole region. An SVD/NN modeling method is then proposed to produce a low-order model from these experiments at all local operation regions. Finally, a practical HPM experiment was used to demonstrate the effectiveness of the proposed method.

1. INTRODUCTION

Hydraulic press machines (HPMs) are crucial to the aviation and transportation industries. As the strength and size of a forging increase, the HPM becomes larger and more complex. It must be able to work across a wide range of velocities (0.005−10 mm/s). Moreover, the resistance of certain material has a strongly nonlinear relation to its deformation and it is difficult to directly express this resistance due to irregular metal flow. All these facts make it difficult to model HPMs accurately. Although many works have discussed first-principle modeling, they neglect a lot of nonlinear factors and some of their assumptions are not satisfied.[1−3] For this reason, only simplified models can be obtained. Moreover, they only consider the dynamic behavior across the local operation region. The resistance of forged materials to deformation is also usually considered to be a linear variable. All these factors can render the first-principle modeling across a large region inaccurate. Data-driven modeling can be used to model such a system. However, no work on this has been published except for a few structural designs for HPM based on finite element analysis.[4,5]

Generally, data-driven modeling methods require that the input spectrum satisfies certain special properties in order to guarantee that the system can be identified.[6−9] These conditions are often difficult to satisfy across a large operation region for practical complex systems when safety and other constraints are taken into account.[10−12] This renders some methods infeasible or undesirable in certain practical applications. For example, large HPMs are unsafe due to their considerable inertia (about 1×10^5 kg) when the velocity of this HPM increases or decreases steeply, and its valve cannot also have a high-frequency action. This makes it difficult for the HPM to produce a required signal, such as the random signal that is often used in data modeling across a large region. Moreover, it is not possible for samples to be collected in sufficient numbers during a single experiment due to the small working distance and the long sampling time. All these issues pose challenges to the modeling of such systems. Thus, a new modeling method will be developed in this paper.

Singular value decomposition (SVD) has found many successful applications, such as the modeling of distribution parameter systems, since it can factorize time-space variables into time variable and space variable.[13−16] It is also used to model system for design because it can factorize output into parameter-space and time-space.[17−19] Moreover, the SVD can produce a low-dimension model from high-dimensional data.[20] It has also been used in feature identification.[21] Here, SVD was used to factorize all experimental data from all local operation regions into time-dependent space and operation-region-dependent space and to reduce the order of the system for the purpose of modeling of the complex HPM.

In this paper, an operation-region-decomposition based SVD/ neural network (NN) modeling method was proposed to model an unknown complex nonlinear system. In this method, a large operation region was first broken down into a group of local operation regions. Every local region was excited by its corresponding local input signal. Then a hybrid SVD/NN modeling method was used to produce a low-order model from experiments conducted at all local operation regions. Finally, a practical HPM experiment was used to demonstrate the effectiveness of the proposed method.

Received: July 10, 2013
Revised: October 25, 2013
Accepted: November 6, 2013
Published: November 6, 2013

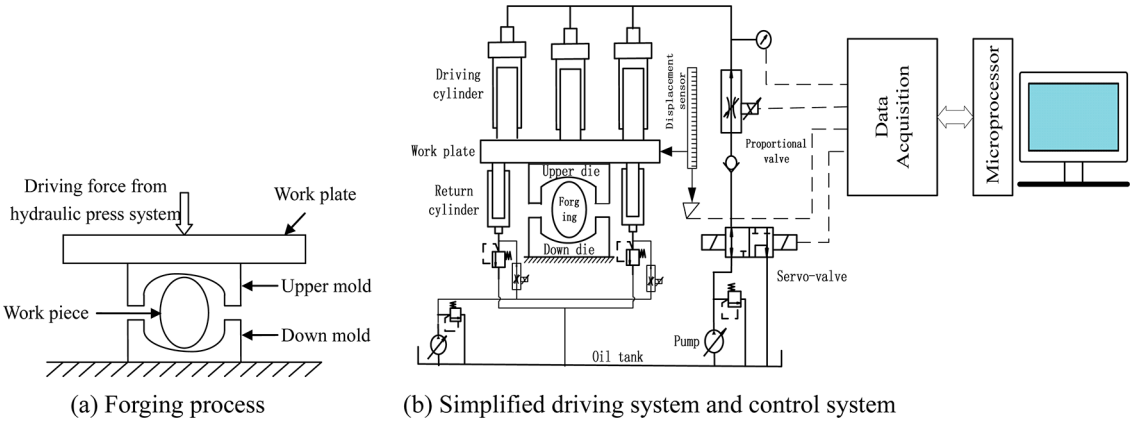

(a) Forging process (b) Simplified driving system and control system

Figure 1. Diagram of an HPM.

2. PROCESS

The 4000T HPM studied here is shown in Figure 1. This HPM offers a forging force to shape a pattern. Because its work plate has considerable inertia (about 1×10^5 kg) and the metal to be forged is often of considerable strength and size, a huge driving force (about 5×10^7 N) is needed for forging. This driving force can be produced by the hydraulic press system, which includes three driving cylinders and four return cylinders. These are located above and below the work plate, respectively. These cylinders are driven by their corresponding hydraulic systems, which consist of pumps, valves, and pipes. A control system is also required to adjust the servo valve of the hydraulic system to achieve a desirable position and velocity for forging.

Producing an accurate model of the HPM is crucial to its prediction and control. However, because the equations describing the flow at the servo valve, pipe, and hydraulic cylinder are nonlinear and the boundary conditions are unknown, they are difficult to obtain accurately. Furthermore, the friction force is inevitable and difficult to model analytically. The resistance of a work piece has a nonlinear relationship with its susceptibility to deformation. This relationship is unknown for two reasons. First, the shape of a piece to be forged is often irregular, and its deformation during forging is also irregular. This makes it difficult to model its resistance to deformation analytically. Second, the resistance depends on material properties, but these material properties are related to stress, the stress ratio, and temperature, which undergo unknown nonlinear variations during forging. Any of these factors could make it difficult to obtain an analytical model of this HPM across a large operation region.

Data-driven modeling is suitable for such systems. However, it requires that the input spectrum have certain special properties within a large operation region in order to guarantee that the system can be identified.[6−9] This is often difficult to obtain due to practical constraints.[10−12] This is especially true of the complex huge HPM. This is for the following reasons: (1) Its valve cannot tolerate a high-frequency action. (2) When the velocity of this HPM increases or decreases sharply, it becomes unsafe due the large amount of inertia generated. (3) Because the displacement of the work plate is small (about 1 m) and the sampling time of the sensor is large (about 1 s), it is prohibitively expensive to collect enough samples for data modeling during a single experiment. (4) It is difficult for the input signal to simultaneously satisfy the requirements of data modeling throughout the large operating region. This poses challenges to the modeling of this system. Thus, a new modeling method must be developed for such a system.

3. MODELING METHOD

A novel modeling method based on operation region decomposition is here proposed. As shown in Figure 2, it has

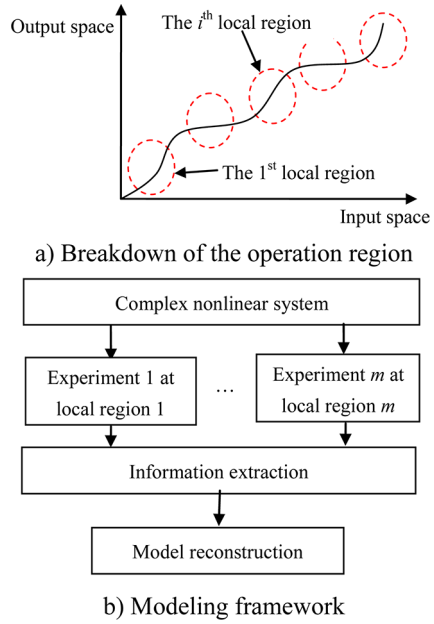

Figure 2. Modeling based on subdivision of the operation.

the following key steps. This large operation region is first broken down into a group of local operation regions. Each local region is excited by its corresponding local input signal. A corresponding experiment is carried out within this local region. Because the system is much less complex within the local region than across the whole operation region, the required input signal for modeling is easier to obtain. This sidesteps the requirement that the input spectrum remain applicable across a large operation region. Then, a low-order model suitable for the design of the controller is built by extracting model information from all these experiments across all local regions.

In this method, the most key issue is to build a low-order model using data from all experiments. Here, a hybrid SVD/NN modeling method, as shown in Figure 3, is proposed to build its low-order model. Because the experimental data from

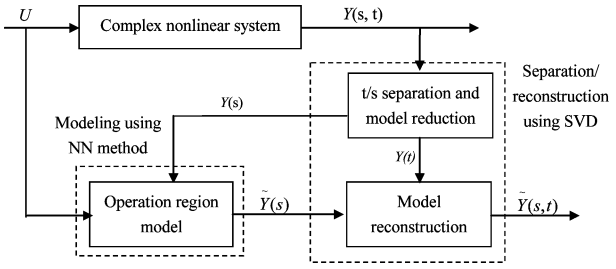

Figure 3. Hybrid SVD/NN modeling framework.

all local operation regions are related to time and the operation region, the SVD method is used to separate them into a time-dependent variable $Y(t)$ and operation-region-dependent variable $Y(s)$. This means that the complexity of the system can be reduced to two parts, $Y(t)$ and $Y(s)$, where t and s represent time and the operation region respectively. Then the nonlinear relationship between $Y(s)$ and its corresponding input U is built using an NN method. Because this relationship only indicates the complexity of the operation-region-dependent variable space and its order is also reduced by SVD, this type of modeling is easier to complete than modeling of the original system. Finally, this system model is reconstructed by synthesizing the NN model obtained in this way and the time-dependent variable. This form of modeling has the following advantages:

(1) It sidesteps the sampling constraints in the large operation region for data modeling. The input signal required for modeling across a local region is easier to obtain than one for modeling across a large region.
(2) It can produce a low-order model suitable for designing controllers.
(3) The model also works well across a large operating region.

A. Data Collection. For the ith experiment at the ith local region, the inputs $U_i = [u_{i,1}\ u_{i,2}\ \cdots\ u_{i,n}]$ and their outputs $Y_i = [y_{i,1}\ y_{i,2}\ \cdots\ y_{i,n}]$ are collected. Here, $y_{i,j}$ and $u_{i,j}$ are the output and input at the time t_j, as shown in Figure 4.

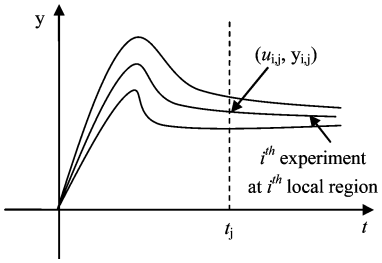

Figure 4. System response in different operation regions.

All response data from all experiments at all local regions are arranged into a matrix $Y(s,t)$:

$$Y(s,\ t) = \begin{bmatrix} y_{1,1} & y_{1,2} & \cdots & y_{1,n} \\ y_{2,1} & y_{2,2} & \cdots & y_{2,n} \\ \vdots & \vdots & \ddots & \vdots \\ y_{m,1} & y_{m,2} & \cdots & y_{m,n} \end{bmatrix} \quad (1)$$

Here, m is the number of local operation regions. Each row of the response matrix represents the discretized time history for a particular experiment at its corresponding local region. Each column corresponds to a particular time step. $U = [U_1\ U_2\ \cdots\ U_m]^T$ is the corresponding input.

B. SVD for *t/s* Separation and Model Reduction. One important nature of the SVD is its factorization ability. Using the SVD, Y may be decomposed as follows:

$$Y(s,\ t) = \tilde{\mathbf{M}}\tilde{\mathbf{S}}\tilde{\mathbf{V}}^T \quad (2)$$

where $\tilde{\mathbf{M}}$ is an $m \times m$ column-orthogonal matrix with each column being the left eigenvector of Y, $\tilde{\mathbf{S}}$ is an $m \times n$ diagonal matrix containing all singular values λ of Y with nonzero singular values equal to r (r less than m and n), $\tilde{\mathbf{V}}$ is an $n \times n$ orthogonal matrix of the right eigenvector of Y.

It is well-known that the system can be approximated by a low-order model if the dominant singular values in $\tilde{\mathbf{S}}$ are considered and the nondominant singular values are neglected. These singular values are expressed as $\lambda_1 > \lambda_2 > \ldots > \lambda_r$. The ratio of the sum of the h largest eigenvalues to the total sum is defined as follows:

$$E = \sum_{i=1}^{h} \lambda_i / \sum_{i=1}^{r} \lambda_i \quad (3)$$

Usually, the number of eigenfunctions sufficient to capture 99% of the system energy is used to determine the value of h. h is decided according to $E > 99\%$.[16] This h is often much smaller than r. In this way, the system is reduced to a low-order model as follows:

$$Y(s,\ t) = \tilde{M}_{m\times h}\tilde{S}_{h\times h}(\tilde{V}_{n\times h})^T \quad (4)$$

Define $\mathbf{D} = \tilde{M}_{m\times h}\tilde{S}_{h\times h}$, $\mathbf{V} = \tilde{V}_{n\times h}$, and then eq 4 may be rewritten as follows:

$$Y(s,\ t) = \mathbf{D}\mathbf{V}^T \quad (5)$$

During the lth experiment, the input signal U_l produces a response $Y_l = Y(s = l,\ t)$. From eq 5, this output can be expressed as follows:

$$Y(s = l,\ t) = d_l\mathbf{V}^T \quad (6)$$

Here, d_l is the lth row of the $\mathbf{D}$ matrix. From eq 6, $Y(s = l,\ t)$ is a linear combination of $\mathbf{V}^T$ and only its weight is variable within the local operation region. In this way, it is clear that different local operation regions have different values of d_l but the same value of $\mathbf{V}^T$. This means that the matrix $\mathbf{D}$ is related to operation region. It is here defined as an operation-region-dependent variable, $Y(s)$.

However, for each point in time t_i, the corresponding input signals in all experiments across the whole operation region produce a response $Y(s,t = t_i)$. Specifically, the outputs of all experiments at time of t_i represent the ith column of the Y matrix. From eq 5, it can be expressed as follows:

$$(Y(s,\ t = t_i))^T = V_i\mathbf{D}^T \quad (7)$$

Here, V_i is the ith row of the V matrix. As shown in 7, $Y(s,t = t_i)$ is a linear combination of $\mathbf{D}$ and only its weight varies over time. In this way, it is clear that different times correspond to different values of V_i but the same value of $\mathbf{D}$. This means that the matrix $\mathbf{V}$ is related to time. It is here defined as a time-dependent variable, $Y(t)$.

In this way, $\mathbf{D}$ is a matrix related to the operation region. Specifically, it is related to the operation-region-dependent information of Y. Moreover, $\mathbf{V}^T$ forms an orthogonal basis of

dx.doi.org/10.1021/ie402189y | Ind. Eng. Chem. Res. 2013, 52, 17221−17228

the response time histories of the various local operation regions, specifically the time-dependent information of Y. This means that the SVD partitions Y into the operation-region-dependent variable $\mathbf{D}$ and time-dependent variable $\mathbf{V}^T$. The details of the mathematical explanation about SVD may also see ref 17.

C. Neural Network Modeling. The $d_i = [d_{i,1}\ d_{i,2}\ \cdots\ d_{i,h}]$ $(i = 1, ..., m)$ within matrix $\mathbf{D}$ are known, while they are unknown at new local experiments that do not used to train the system model. For prediction and control, this d_i must be obtained during the experiment in the arbitrary local region.

Generally, when the model structure of a system is unknown and strongly nonlinear, the use of neural networks (NNs) is an advisable means of producing a model of this system using input/output data. It has been proven that it may approximate any nonlinear system well and has many successful applications.[22−24] Here, a NN method was used to model the following unknown model f from the input data $U = [U_1\ U_2\ \cdots\ U_m]^T$ and the output data $D = [d_1\ \cdots\ d_m]^T$, as shown in Figure 5.

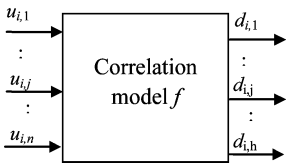

Figure 5. Correlation model f.

$$d_i = f(U_i) \tag{8}$$

Here, f is approximated by a radial basis function (RBF) network $\tilde{f}$, as shown in Figure 6, due to its strong modeling ability and well-developed theory.

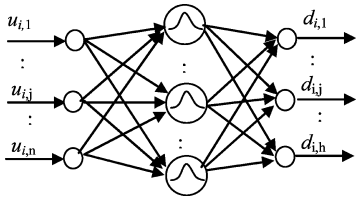

Figure 6. Neural network modeling.

$$\tilde{f}(U_i) = W_i\phi(U_i) \tag{9}$$

Here, $W_i = [w_{i,1}\ w_{i,2}\ \cdots\ w_{i,l}] \in R^{m\times l}$ denotes the weight, $\phi(\bullet) = [\phi_1\ \phi_2\ \cdots\ \phi_l]$ denotes the radial basis function, and l is the number of neurons. The radial basis function is often selected as the Gaussian function $\phi_j(U_i) = \exp(-(U_i - c_{ij})^T\Sigma_j^{-1}(U_i - c_{ij})/2)$ with a proper center vector c_{ij} and a norm matrix Σ_j $(j = 1, ..., l)$.

There are many mature algorithms for training the RBF network, most of which first determine the parameters c_{ij} and Σ_j, and unknown weight W_i can then be estimated using the recursive least-squares method.[23]

D. Model Reconstruction. As shown in section B, different local operation regions correspond to different d but with the same $\mathbf{V}^T$. This means that, when the system works at different local operation regions, their time-dependent variable $\mathbf{V}$ stays the same and constructs a time basis function, but their operation-region-dependent variables differ. The aforementioned NN modeling can be used to estimate the operation-region-dependent variable in arbitrary local region very effectively. In this way, the system model at arbitrary local region can be reconstructed by synthesizing the time-dependent variable $\mathbf{V}^T$ and its corresponding operation-region-dependent variable d_i. Thus, the response output of the system excited by the input $\bar{u}_i$ is modeled as follows:

$$\tilde{y}(\bar{u}_i) = \tilde{d}_i\mathbf{V}^T = \tilde{f}(\bar{u}_i)\mathbf{V}^T \tag{10}$$

where the vector $\tilde{d}_i$ is an estimation of the operation-region-dependent variable vector d_i corresponding to $\bar{u}_i$.

From this model, the required input signal for modeling at a local region is easier to obtain than the one in a large operation region, and the experiment is easier to perform across the local region than across the whole operation region. This allows the system to sidestep the requirement for input spectra with special properties across a large operation region. More importantly, the proposed method can extract model information from all experiments at all local operation regions effectively and has a low-order model.

For a multi-input and multi-output system, each output is arranged into a matrix $Y(s, t)$ and then the proposed method is used to obtain its model as the same with modeling of a single-input and single-output system. In this way, the modeling of the multioutput system is transformed into the modeling of many single-output systems, like many common data modeling methods to handle multi-input and multioutput systems.

The proposed method is also different from the Wiener and Hammerstein models: (1) It breaks down a system that has a large operation region into many subsystems with local operation regions, and the Wiener and the Hammerstein models break down the system into a linear dynamic and a static nonlinear model. (2) Its model structure is the product of two parts, as presented in eq 10, but the other two models are the sum of both a linear dynamic model and a static nonlinear model.

4. EXPERIMENT VERIFICATION

Experiments were performed on a practical 4000T HPM, as indicated in Figure 7, to confirm the effectiveness of the proposed method. In the present study, the input of the HPM is the pressure of the cylinders and its output is the

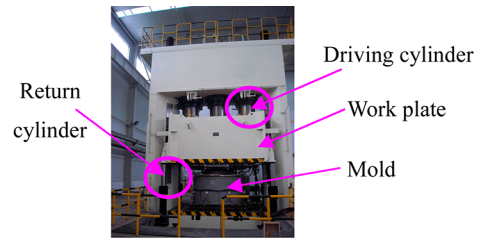

(a) 4000T HPM

(b) Control panel figure

(c) Data collection system

Figure 7. Practical 4000T HPM.

dx.doi.org/10.1021/ie402189y | Ind. Eng. Chem. Res. 2013, 52, 17221−17228

displacement of the work plate. The shapes of the work piece before and after forging are shown in Figure 8a and b,

(a) Initial shape (b) Final shape

Figure 8. Materials before and after forging.

respectively. The length, width, and height of the material to be forged were 570, 100, and 90 mm, respectively, and this material was aluminum alloy (AL-1100).

The pressure and displacement at different velocity regions (0.005−1 mm/s) are as shown in Figure 9, where a sample was

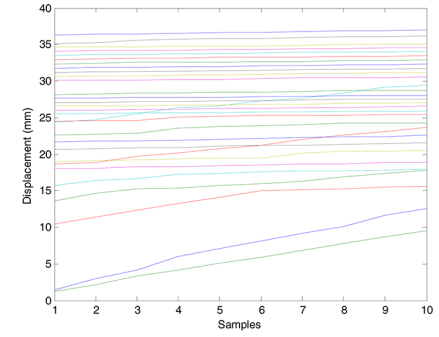

a) Displacement samples

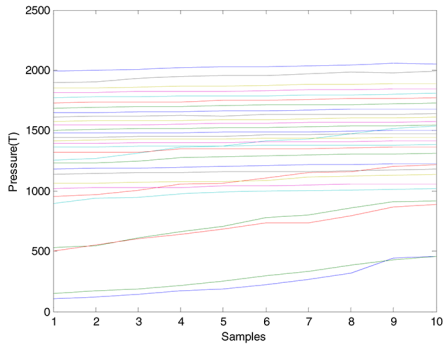

b) Pressure samples

Figure 9. Input and output samples for training.

collected over the course of one second. In Figure 9, each line represents an experiment and each experiment ran at a certain velocity. In this way, the gradient of each experiment line represents a corresponding velocity. From this figure, it is clear that an experiment, namely a line in Figure 9, only incorporates a small part of the information regarding the dynamics of the system. If the model of the system is obtained from an experiment, it produces a large modeling error. The objective of this modeling process is to produce a model of the system from multiple experiments in different operation regions. In this way, the pressure and the displacement serve as the input and the output respectively. They are first used to train the model using the proposed method. All inputs and all outputs are arranged into matrices **U** and **Y**, respectively, and SVD is performed for output matrix **Y**. From this, its singular values are obtained, as shown in the Appendix. Because of $\sum_{i=1}^{4}\lambda_i/\sum_{i=1}^{10}\lambda_i = 0.995$ in matrix $\tilde{\mathbf{S}}$, h is equal to 4 and the fourth-order model is used to express this HPM system. The corresponding matrices **D** and **V** are obtained as shown in the Appendix.

Then, the RBF network is used to model $\mathbf{D} = \tilde{f}(\mathbf{U})$ from data sets **U** and **D**. This network creates a two layer network. The first layer has RADBAS neurons. The second layer has PURELIN neurons. Both layers have biases. All of them, including training algorithm, are available in the neural network toolbox in MATLAB. Finally, after obtaining **V** and $\mathbf{D} = \tilde{f}(\mathbf{U})$, the model of the system is reconstructed as follows:

$$\tilde{y}(\overline{u}_i) = \tilde{f}(\overline{u}_i)\mathbf{V}^{\mathrm{T}} \tag{11}$$

A. Verification with Training Samples. First, the training samples are used to confirm the proposed method. Outputs of two training experiments are shown in Figures 10 and 11.

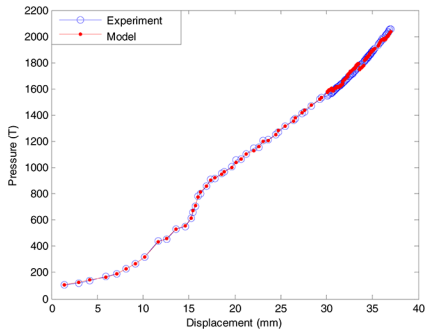

Figure 10. First training experiment.

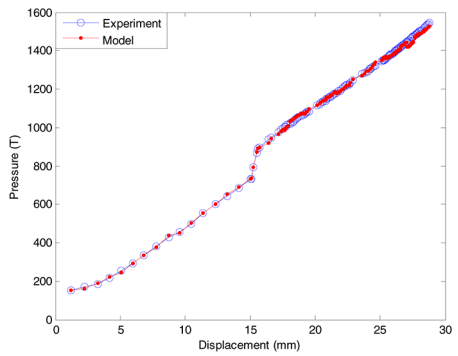

Figure 11. Second training experiment.

They are indicated with lines marked with circles. Using the same input data with these two training experiments, the output data of the estimated model (eq 11) are represented by the dotted lines in Figures 10 and 11. These two figures show that this model fits these experiments well. In this way, the proposed modeling method is an effective means of producing a model of the complex nonlinear system.

B. Verification with Test Samples. The test samples were used to confirm the effectiveness of the model. A new experiment was designed for this test. This experiment differed from the aforementioned experiments used for modeling (eq 11). The relative error is defined as follows:

$$\text{relative error}\ (\%) = \frac{\text{experimental output} - \text{estimated output}}{\text{experimental output}} \times 100 \tag{12}$$

dx.doi.org/10.1021/ie402189y | Ind. Eng. Chem. Res. 2013, 52, 17221−17228

This relative error is used to show the precision of the modeling process. The smaller it is, the more accurate the model.

The output data of the test experiment is shown in Figure 12a as lines marked with circles, and the output data of the model is

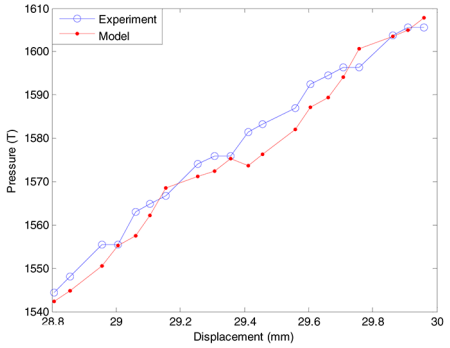

(a) Experiment and model

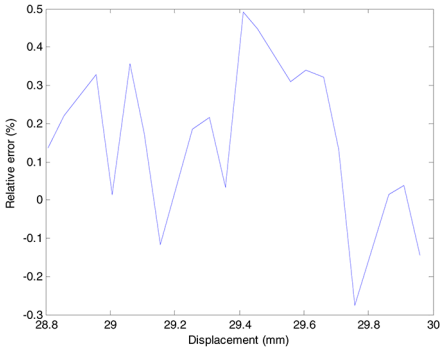

(b) Relative error

Figure 12. Test samples.

represented by the dotted line. Figure 12a shows that the data model (eq 11) matches the experiment closely. The relative error between the experiment and the model is shown in Figure 12b. Figure 12 shows that this model is closely consistent with the output as observed under practical circumstances, as indicated by the small relative error, which is below 0.5%.

In summary, through verification of both training samples and test samples, the proposed method was found to be an effective means of producing a model of the system from all experiments within all local operation regions.

C. Comparison to Two Common Methods. The effectiveness of the proposed modeling method was demonstrated through comparison to the first-principle modeling method and the RBF network method.[3,25] Here, the first-principle modeling method was derived from the force balance of the work plate. However, it neglected the nonlinear term and only used a second-order linear model to express the system. The RBF network model was obtained from experimental data. This network also creates a two layer network. The first layer has RADBAS neurons. The second layer has PURELIN neurons. Both layers have biases. The input/output data at this experiment is respectively shown in Figure 13a and b. They were used to train the RBF network model.

Finally, the root-mean-square error (RMSE) was used to estimate the performance of the proposed modeling method, the RBF network modeling method, and the first-principle

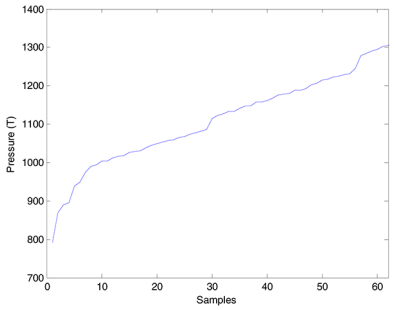

(a) Pressure for input

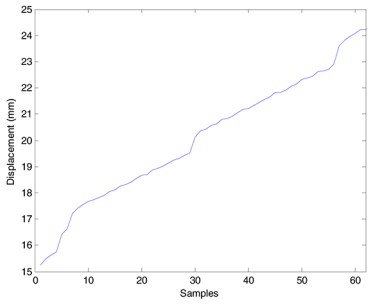

(b) Displacement for output

Figure 13. Input and output data for RBF network.

modeling method. The RMSE results produced using the training and test samples are shown in Table 1, from which the

Table 1. Performance

	RMSE with training samples	RMSE with test samples
new method	0.76	0.89
first-principle modeling method	0.81	1.25
NN method	0.808	11.7

RMSE obtained by the proposed method is smallest than the other two methods. Thus, the proposed method has a better performance than the other ones. This is because the proposed method considers the system information across the whole operation region, and the first-principle modeling method neglects the nonlinear influence, and the RBF network is suitable to work across a local region.

5. CONCLUSION

An operation-region-decomposition-based SVD/NN modeling method was proposed for a complex nonlinear system. Because the system is much less complex within local regions than the original system that is across the whole operation region, the required input signal for modeling within a local region is easier to obtain than one suitable for use across a large region. The proposed hybrid SVD/NN modeling method could extract model information from all these experiments at all local regions very effectively. It may also reconstruct a model of the complex nonlinear system working in a large operation region well. The model built here was low-order, which makes it easier to design a controller. Experiments on the HPM also demonstrated the effectiveness of the proposed method.

APPENDIX

$$[\lambda_1 \cdots \lambda_{10}] = [2.46\ 0.0799\ 0.011\ 0.0052\ 0.0034\ 0.002\ 0.002\ 0.001\ 0.001\ 0.0009] \times 10^4$$

$$V = \begin{bmatrix} -0.30804738683349 & -0.46253672565444 & 0.43782696785508 & -0.44474234292113 \\ -0.30961715498650 & -0.39217568982207 & 0.28141022385523 & 0.21516297394778 \\ -0.31182329805839 & -0.28772793314597 & 0.01449689193381 & 0.18839019788793 \\ -0.31403064867300 & -0.17045706161051 & -0.24516966873915 & 0.26540012453416 \\ -0.31528184811489 & -0.08610511272723 & -0.36143625297915 & 0.30185705455065 \\ -0.31733545584721 & 0.04717886991099 & -0.43565391340728 & 0.07566958124548 \\ -0.31882585756888 & 0.11952499470537 & -0.23237042075877 & -0.54685259799383 \\ -0.32059401649027 & 0.25219886965100 & -0.17732463244654 & -0.42895297686109 \\ -0.32268362142262 & 0.44274108406818 & 0.33223270715560 & 0.18478812118856 \\ -0.32362849318053 & 0.48668771756624 & 0.39057444761356 & 0.18958484475591 \end{bmatrix}$$

$$D = \begin{bmatrix} -0.77399544209250 & 0.35534610580954 & 0.07932256997090 & 0.00907895555365 \\ -2.32147215935819 & 0.38749296734451 & -0.04301872612798 & -0.01906368788108 \\ -3.44626770078626 & 0.22393361483746 & -0.01869813656632 & -0.01227384329922 \\ -4.41202770135920 & 0.22338285862770 & -0.00843985206798 & 0.00471979457825 \\ -4.93179444894121 & -0.05104107034898 & 0.00489226162813 & 0.00281871685652 \\ -5.03318345621145 & -0.04674150131542 & 0.00807309879494 & 0.00050168907271 \\ -5.14904423791658 & -0.05369967239677 & 0.00434803732752 & -0.00197585382767 \\ -5.26272292144763 & -0.05010989383162 & 0.00391294554211 & 0.00007133925303 \\ -5.39922740611772 & -0.04768976801426 & 0.00300767688916 & 0.00194468023964 \\ -5.53103788632199 & -0.04572341118776 & 0.00384062223531 & -0.00231334607777 \\ -5.66031474409437 & -0.05520661150989 & 0.00734291871256 & 0.00113183222160 \\ -5.78675915147722 & -0.05913745998820 & 0.00730358883503 & 0.00000006263217 \\ -5.92212346293251 & -0.05460078357300 & 0.00697457031010 & -0.00223475684676 \\ -6.17237120440201 & -0.01037477244120 & -0.01463727179032 & -0.00097091715698 \\ -6.40908574235578 & 0.03876967917403 & 0.00361972126983 & 0.00223708239901 \\ -0.91514637170539 & 0.31334751166998 & 0.01990205448424 & -0.02010203703814 \\ -2.21889241323286 & 0.34811989573205 & -0.01585813999281 & 0.03342872251683 \\ -3.09395134672784 & 0.05620697416405 & -0.03712946739489 & 0.01528665268065 \\ -3.29020098834748 & -0.01014241925146 & 0.00121676999019 & -0.00167744991684 \\ -3.46289138002692 & 0.02164838768725 & 0.01334413868832 & -0.01486260503627 \\ -3.65791530888411 & -0.01584233886904 & 0.00381971650752 & 0.00455867723798 \\ -3.80669818466056 & -0.01484665862147 & 0.00160453244161 & -0.00248506832379 \\ -4.03983044988434 & 0.02139561645139 & -0.02400195691717 & -0.00035467254800 \\ -4.24937467587112 & -0.02190074319066 & -0.00957684718025 & 0.00474209864553 \\ -4.34789121099964 & -0.05005094034700 & 0.00109449544855 & 0.00122122089160 \\ -4.43700947787404 & -0.04375755599050 & 0.00495804975870 & 0.00136335265780 \\ -4.52541667737021 & -0.04583245819370 & 0.00390426819980 & 0.00317591178707 \\ -4.61567224097783 & -0.04189546913894 & 0.00569679144611 & -0.00484865234757 \\ -4.70802242446439 & -0.05305055349414 & 0.01046054848699 & 0.00016663502758 \\ -4.82303336453526 & -0.04043609309405 & 0.00335633868673 & 0.00093287951077 \end{bmatrix} \times 10^3$$

dx.doi.org/10.1021/ie402189y | Ind. Eng. Chem. Res. 2013, 52, 17221−17228

AUTHOR INFORMATION

Corresponding Author

*E-mail: csumeel@gmail.com.

Notes

The authors declare no competing financial interest.

ACKNOWLEDGMENTS

The paper was partially supported by the National Basic Research Program (973) of China under Grant (2011CB706802), National Natural Science Foundation of China (51205420), Program for New Century Excellent Talents in University (NCET-13-0593), Fund for the State Key Laboratory of High Performance Complex Manufacturing and the State Key Laboratory of Metal Extrusion and Forging Equipment Technology.

REFERENCES

(1) Cho, S. J.; Lee, J. C.; Jeon, Y. H.; Jeon, J. W. The Development of a Position Conversion Controller for Hydraulic Press Systems. *Proceedings of the 2009 IEEE International Conference on Robotics and Biomimetics*, China, Dec. 19−23, 2009.

(2) Chen, M.; Huang, M. H.; Zhou, Y. C.; Zhan, L. H. Synchronism Control System of Heavy Hydraulic Press. *IEEE International Conference on Measuring Technology and Mechatronics Automation*, China, Jan. 16−17, 2009.

(3) Lu, X. J.; Huang, M. H. System decomposition based multi-level control for hydraulic press machine. *IEEE Trans. Ind. Electr.* **2012**, *59* (4), 1980−1987.

(4) Zhu, P. H.; Zhang, L.; Zhou, R.; Chen, L.; Yu, B.; Xie, Q. A Novel Sensitivity Analysis Method in Structural Performance of Hydraulic Press. *Math. Problems Eng.* **2012**, *2012*, 1−21.

(5) Liu, Q.; Bian, X. Multi-objective optimization of the hydraulic press crossbeam based on neural network and pareto GA. *2010 2nd International Conference on Advanced Computer Control (ICACC)*, China, March 27−29, 2010; Vol. *1*, pp 52−55.

(6) Soderstrom, T.; Stoica, P. *System identification*; Prentice Hall International (UK) Ltd, 1989.

(7) Overschee, P. V.; Moor, B. D. *Subspace identification for linear systems: theory, implementation, applications*; Kluwer Academic Publishers: Boston, 1996.

(8) Dai, S. L.; Wang, C.; Luo, F. Identification and Learning Control of Ocean Surface Ship Using Neural Networks. *IEEE Trans. Ind. Infor.* **2012**, *8* (4), 801−810.

(9) Jeon, S. H.; Oh, K. K.; Choi, J. Y. Flux observer with online tuning of stator and rotor resistances for induction motors. *IEEE Trans. Ind. Electr.* **2002**, *49* (3), 653−664.

(10) Lozano, R.; Zhao, X.-H. Adaptive pole placement without excitation probing signals. *IEEE Trans. Automatic Control* **1994**, *39* (1), 47−58.

(11) Marafioti, G.; RBitmead, R.; Hovd, M. Persistently exciting model predictive control using fir models. *International Conference Cybernetics and Informatics*, Slovak Republic, Feb. 10−13, 2010.

(12) Lu, X. J.; Li, H. X. Sub-domain intelligent modeling based on neural networks. *IEEE International Joint Conference on Neural Networks*, Hong Kong, June 1−6, 2008; pp 445−449.

(13) Qi, C. K.; Li, H.-X.; Li, S. Y.; Zhao, X. C.; Gao, F. Kernel-Based Spatiotemporal Multimodeling for Nonlinear Distributed Parameter Industrial Processes. *Ind. Eng. Chem. Res.* **2012**, *51* (40), 13205−13218.

(14) Qi, C. K.; Li, H.-X.; Li, S. Y.; Zhao, X. C.; Gao, F. Probabilistic PCA-Based Spatiotemporal Multimodeling for Nonlinear Distributed Parameter Processes. *Ind. Eng. Chem. Res.* **2012**, *51* (19), 6811−6822.

(15) Zheng, D.; Hoo, K. A.; Piovoso, M. J. Low-order model identification of distributed parameter systems by a combination of singular value decomposition and the Karhunen-Loève expansion. *Ind. Eng. Chem. Res.* **2002**, *41* (6), 1545−1556.

(16) Li, H. X.; Qi, C. K. Modeling of Distributed Parameter Systems for Applications−A Synthesized Review from Time-Space Separation. *J. Process Control* **2010**, *20* (8), 891−901.

(17) Seecharan, T. S. *Probabilistic Robust Design for Dynamic Systems Using Metamodelling*. Master thesis, University of Waterloo, 2007.

(18) Wehrwein, D.; Mourelatos, Z. P. Reliability-Based Design Optimization of Vehicle Drivetrain Dynamic Performance. *Int. J. Product Dev.* **2008**, *5* (1−2), 54−75.

(19) Wehrwein, D.; Mourelatos, Z. P. Optimization of engine torque management under uncertainty for vehicle driveline clunk using time-dependent metamodels. *J. Mech. Design* **2009**, *131*, 051001.

(20) Berrar, D. P.; Dubitzky, W.; Granzow, M. *A Practical Approach to Microarray Data Analysis*; Kluwer Academic Publishers: Boston, 2003.

(21) Zhou, J. H.; Pang, C. K.; Lewis, F. L.; Zhong, Z. W. Intelligent Diagnosis and Prognosis of Tool Wear Using Dominant Feature Identification. *IEEE Trans. Ind. Inform.* **2009**, *5* (4), 454−464.

(22) Mathieu, D. Power Law Expressions for Predicting Lower and Upper Flammability Limit Temperatures. *Ind. Eng. Chem. Res.* **2013**, *52* (26), 9317−9322.

(23) Ge, Z. Q.; Song, Z. H.; Gao, F. R. Review of Recent Research on Data-Based Process Monitoring. *Ind. Eng. Chem. Res.* **2013**, *52* (10), 3543−3562.

(24) Jiang, Z. J.; Yang, Y.; Mo, S. Y.; Yao, K.; Gao, F. R. Polymer Extrusion: From Control System Design to Product Quality. *Ind. Eng. Chem. Res.* **2012**, *51* (45), 14759−14770.

(25) Huang, M. H.; Li, Y. B.; Zhang, M.; Yang, J. W. Dynamic performance analysis for die-forging press machine under extremely low speed. *J. Central South Univ.* **2012**, *43* (11), 1672−7207.